Tue-Af-Po2

High definition 3D finite element analysis of low temperature Rutherford cable

Tarik Plomion [1], François Nunio [1], Pierre Manil[1]

[1] CEA Paris-Saclay/IRFU, France

In the perspective of simulating and managing the mechanical stresses within strain-sensitive superconductors such as Nb_3Sn, we are proposing a multiscale numerical approach for 3D simulation of Rutherford cables, up to the filament scale. It opens the way to the prediction of coil electromagnetic performance in 3D.

The cable mesh is built over a transposition pitch within a **simplified cabling process model** B1 (pre-processor) [1]. Periodic boundary conditions allow to build longer cable meshes, that can be used for the **3D Finite Element mechanical calculation of the cable in service** B2.

Both models (cabling and service) rely on a bi-metallic description of the strands. Several geometrical options for the modeling of the strand annular topology are used. The material behavior law of each component is obtained experimentally at the microstructure level [2]. **Material properties are homogenized in 3D** A. Up to now, elastoplastic values at room temperature are used, without cycling.

Multiscale post-processing C allows the inclusion of a high definition three-dimensional sub-modelling of the strand geometry, up to the superconducting filaments scale. Options for the description of the strand topology are compared on the basis of these models.

The strain/stress map on the superconducting filaments can be used to compute the **critical current degradation** using existing scaling laws [4],[5].

CONCLUSIONS

This multiscale approach has allowed us to bridge 3D mechanical models at the cable level to the estimation of strain/stress map on the superconducting filaments, which drives the cable current transport capability. **In the future, after obtaining cryogenic material properties, the full loop will be cross-checked with experimental critical current measurements on a cable under transverse pressure** [6].

A Homogeneization of the elastoplastic mechanical properties of the filament bundle region composed of copper, tin and Nb_3Sn filaments (based on room temperature measurements [2])

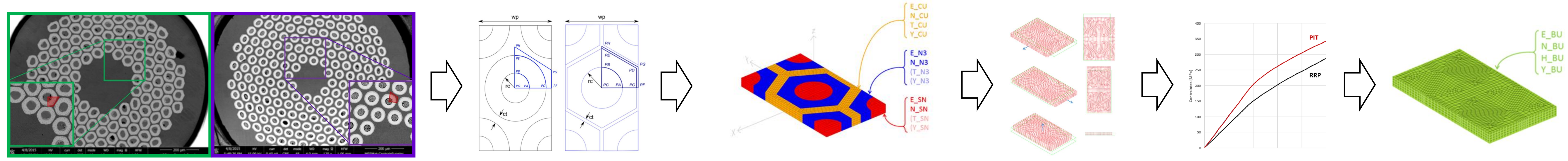

a. Identification and characterization of the **Representative Volume Element** for each type of strand [2]

b. Modeling and meshing of the Representative Volume Element of PIT and RRP strands

c. Implementation of the elastoplastic mechanical properties (copper, Nb_3Sn and 'dummy tin')

d. Numerical traction tests (2 methods)

e. Numerical mechanical behaviour of PIT and RRP strands (transverse)

f. Identification of the **homogenized properties of the bundle region**

B1 Pre-processor: simplified cabling model

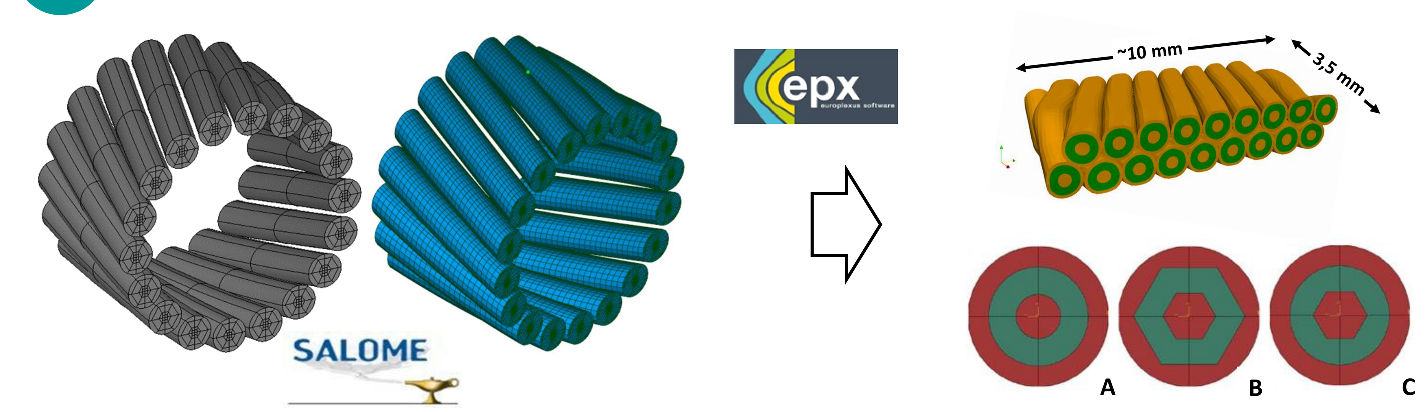

a. Generation of the simpified mesh of one transposition pitch of 18-strand cable, **before cabling**, at the strand level (**bi-metallic model**)

b. **3D cabling model** based on explicit formulation [1], valiated by automated comparison to tomographic data [3]

B2 3D FEM model of cable in service | Transverse compression test on 18-strand Rutherford cable

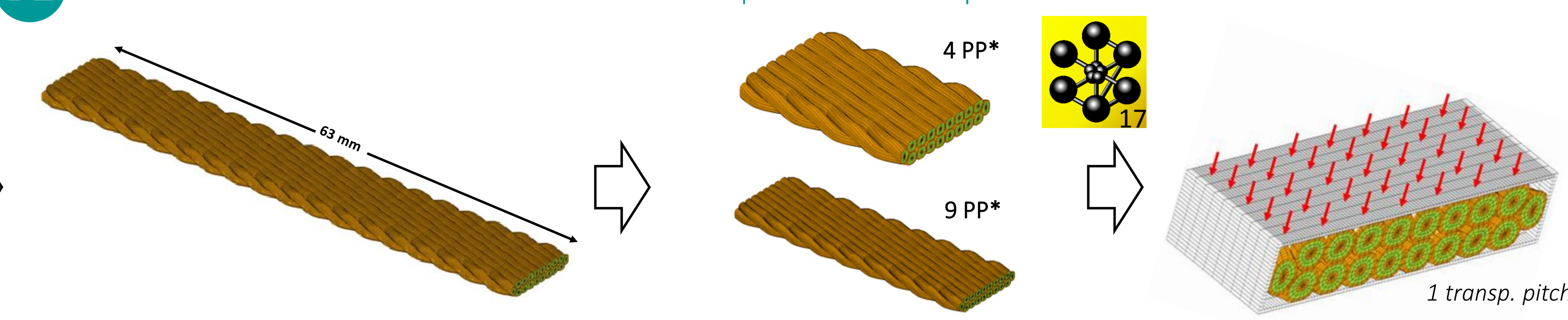

c. Construction of the **full twist pitch** (or any length) of a cable (based on periodic bounadary conditions)

d. Preparation of the mechanical model (cable configuration and length, environment…)

e. **3D numerical simulation** of transverse pressure over a cable

C Mutiscale post-treatment up to the superconducting filaments scale

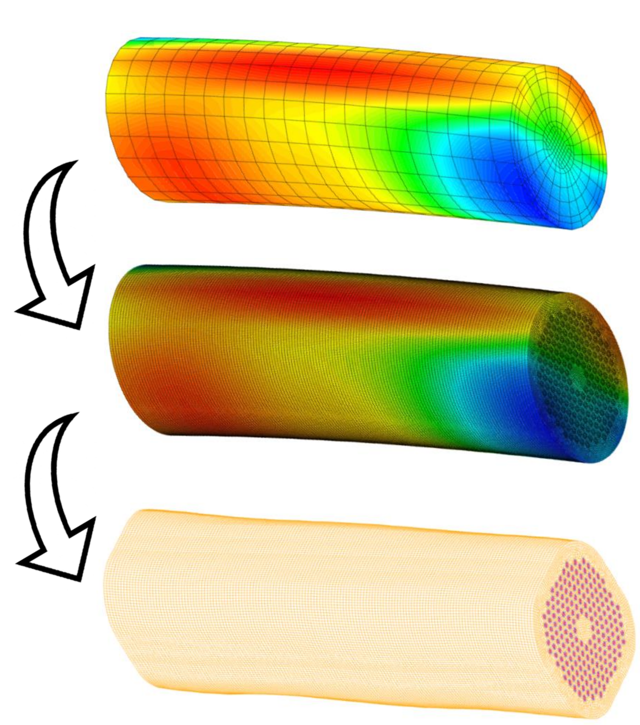

a. **Projection of the strain field** extracted from the cabling model B1 over the detailed mesh of any strand (no additional calculation)

c. Export of the **3D strain/stress maps** on the detailed mesh of any strand

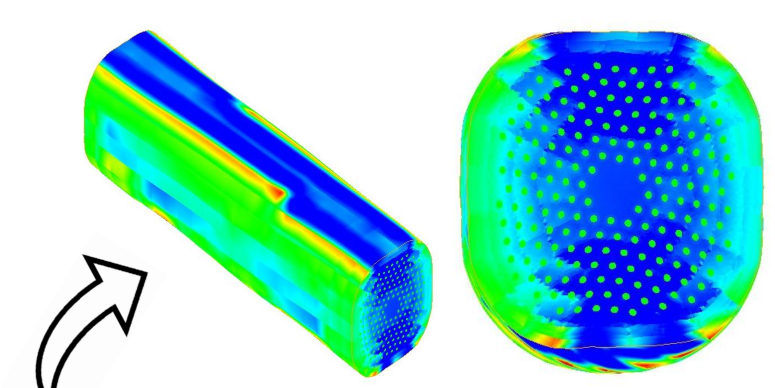

b. **Second projection of the strain field** extracted from the mechanical model B2 over this deformed detailed mesh

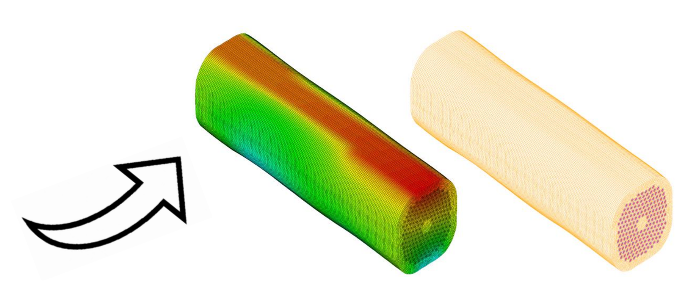

Only Nb_3Sn filaments are considered for post-treatment

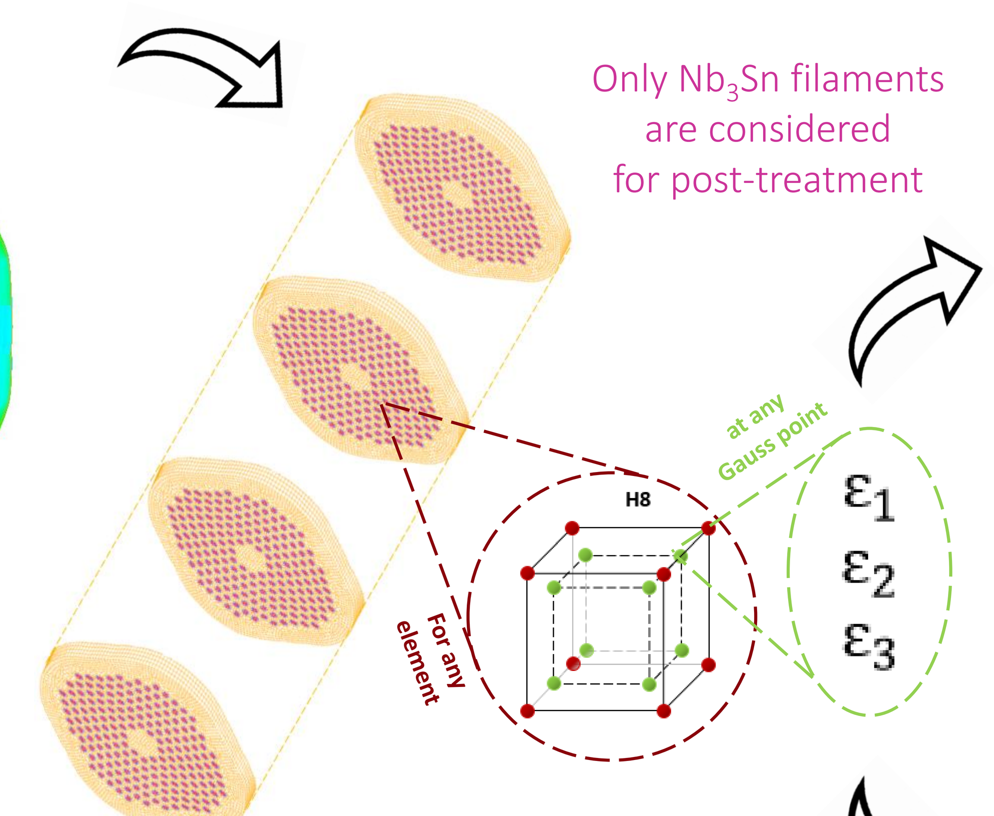

d. Subdivision of the detailed mesh into several slices

Principal strain distribution within PIT strand (one component shown)

Plots A, B, C refer to the geometrical cofigurations described in B1b.

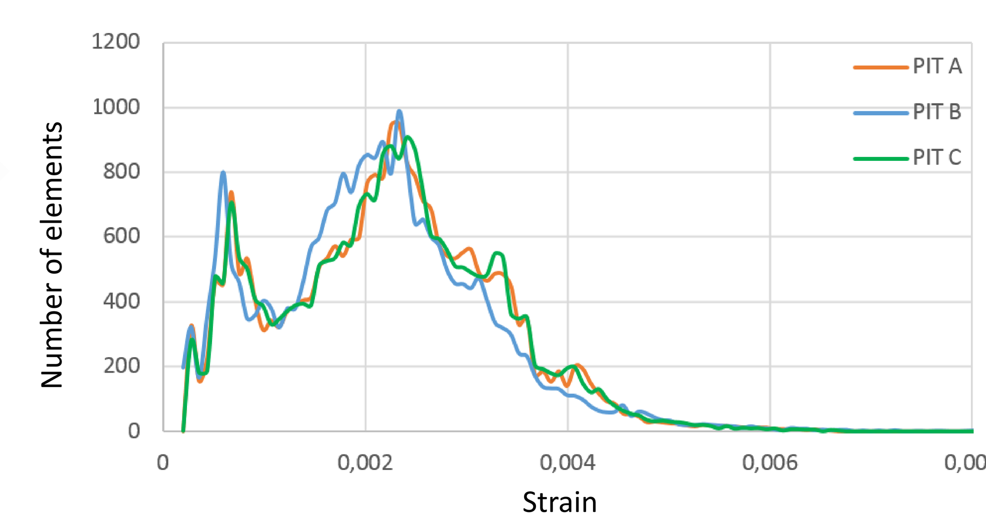

Critical current degradation can be computed for each element using existing scaling laws [4],[5] **and summed up on the whole domain**

$$\varepsilon_1, \varepsilon_2, \varepsilon_3 \Rightarrow I1 = \mathrm{tr}(\varepsilon),\quad J2 = \frac{1}{2}\left[\left(\mathrm{tr}(\varepsilon_D)\right)^2 - \left(\mathrm{tr}(\varepsilon_D)\right)^2\right] \Rightarrow T_c(\varepsilon),\ B_{c2}(T,\varepsilon),\ F_p(T,\varepsilon) \Rightarrow Ri \Rightarrow \frac{I_c}{I_{c0}} = \frac{\sum_{i=1}^{N} A_i R_i}{\sum_{i=1}^{N} A_i}$$

Cross-check with experimental data is planned [6]

References (details can be found on the poster board):
[1] Manil, *IEEE*, 2017 [2] Lenoir, *PhD thesis*, 2017 [3] Lermé, *IPCRAM*, 2016
[4] Bordini, *IEEE*, 2013 [5] Wang, *Cryogenics*, 2014 [6] Bordini, *IEEE*, 2014

This work has been conducted within the framework of the French ANR-funded project CoCaSCOPE (grant ANRGUI-AAP-05) | Cable samples have been provided by CERN

Direction de la recherche fondamentale
Institut de recherche sur les lois fondamentales de l'Univers